51st AIAA/SAE/ASEE Joint Propulsion Conference, July 27–29, Orlando, Florida

Multiple-Kilowatt-Class Graphite Heater for Large Hollow Cathode Ignition

Christopher J. Wordingham,* Pierre-Yves C. R. Taunay,†

Edgar Y. Choueiri‡

Electric Propulsion and Plasma Dynamics Laboratory

Princeton University, Princeton, NJ 08544 USA

A graphite heater design capable of operating in the multiple-kilowatt power range with an estimated life of over 40 years of continuous operation has been developed to address the power and operational life requirements of large lanthanum hexaboride hollow cathodes. Larger hollow cathodes are capable of increased discharge currents, but require higher heater powers to ignite. Legacy heater designs suffer from material interactions and increased failure rates at high temperatures and are currently not viable for high-power operation; a graphite heater can provide high power and long operational life simultaneously. Two models, a simplified circuit model and a finite-element model, have been developed to predict the operating temperature and resistance of the graphite heater design. The sublimation-limited operational life of the heater was estimated using a Hertz-Knudsen evaporation model and an alternate vacuum sublimation model proposed by Thieberger. A prototype heater has been fabricated and tested using a large-diameter lanthanum hexaboride hollow cathode to demonstrate the feasibility of the graphite heater design. The prototype has repeatedly achieved cathode ignition and has been tested at up to 4.5 kW of heater power. The temperatures of the cathode and heater element were measured during heating prior to ignition and used to calculate the heater resistance, which was found to agree fairly well with the predicted values. The exposed portion of the heater element and the cathode tube tip reached temperatures of just over 1300 and 1200°C, respectively. For a peak surface operating temperature of 1500°C, both heater sublimation life models predict a 1% loss life of approximately 400 kh.

I. Introduction

The next generation of high-power Hall thrusters for use in manned and cargo missions is expected to operate at discharge powers ranging from 100 to 200 kW.[1] These thrusters will require cathodes capable of discharge currents ranging from 300 to 700 A that can operate for 100 kh,[2,3] outpacing the capabilities of state-of-the-art hollow cathodes. Larger hollow cathodes are candidates for high-power thruster operation, but require significantly more heater power to reach emission temperatures.[4] Therefore, reliable, high-power heaters should be developed.

Legacy heater designs for hollow cathodes are typically manufactured using swaged tantalum with either alumina or magnesium oxide (MgO) insulation.[2,5–8] The electrical resistivity of both of these insulation materials decreases with temperature,[9] and in the case of MgO, the decrease is so significant as to limit its use to dispenser cathodes operating at temperatures less than 1400°C.[2] Furthermore, these heaters have the tendency to form voids in the MgO insulation during the swaging process which can lead to thermal runaway or breakdown failure of the heater insulation and therefore require thermal cycle testing to determine the risk they pose to heater life.[9] Finally, tantalum can also diffuse through and react with the

*Graduate Research Assistant, EPPDyL; Mechanical and Aerospace Engineering Dept., Student Member AIAA.

†Graduate Research Assistant, EPPDyL; Mechanical and Aerospace Engineering Dept.

‡Chief Scientist, EPPDyL; Professor, Applied Physics Group, Mechanical and Aerospace Engineering Dept.; Fellow AIAA.

MgO insulation, creating conductive paths that may eventually lead to heater failure.[10] These risks may be further exacerbated during higher-power operation.

Though alumina-insulated heaters have been successfully used for many cathodes and can operate at temperatures between 1600 and 1800°C depending on the material used,[2,8,11] they still face many of the same issues as their MgO-insulated counterparts. These heaters have demonstrated "excellent life" for limited heater currents,[2] but an increase in current of less than 10% of the nominal value can reduce the lifetime of the heater to less than 100 hours.[8] This sensitivity to operating conditions is also shown in MgO-insulated heaters.[10] The failure mechanisms for alumina-insulated heaters include continued sintering during operation that leads to grain growth and void formation,[8] and melting of the heater material during cathode operation due to orifice temperatures exceeding 2000°C.[5] Neither tantalum nor molybdenum, with melting points of 2996 and 2620°C, respectively,[12] should be melting at the temperatures reached by the cathode at the heater location. Therefore, it seems likely that an interaction between the cathode tube and heater materials is at fault. The authors propose that the melting is due to Mo-Ta eutectic formation,[5] but this has not been reported in previous work regarding the binary Mo-Ta system.[13–15] Pure alumina does, however, melt at 2050°C,[12] and the maximum use temperature for alumina is typically restricted to 1750°C.[11] Commercial additives and grain size refinement can also reduce the melting temperature of alumina to the 1700 to 1850°C range.[12]

All of the aforementioned problems with swaged heaters have been experienced at power levels much less than a kilowatt, with the highest reported heater power required for operation being approximately 400 W.[6] The anticipated power requirement for larger hollow cathodes is in the multiple-kilowatt range,[4] due to a larger cathode tube and wall thicknesses. Therefore, an alternative to legacy heater designs is desirable. Prior testing of a 2.7-cm-inner-diameter, lanthanum hexaboride (LaB_6) hollow cathode by Plasek et al.[4] relied on bare tungsten wire heaters insulated from the cathode tube by boron nitride rings, with or without carbon beads around the tungsten wire to prevent interactions between the wire and the boron nitride. These heaters consistently suffered structural failure due to one or all of the following: arcing or plasma attachment to the heater coil, boride formation, recrystallization embrittlement, localized melting, and possibly even carburization.[4]

One of the primary problems for any refractory metal heater is recrystallization, which causes the metal to lose much of its ductility and to become brittle. Recrystallization occurs at high temperatures and takes place for tungsten, molybdenum, and tantalum at a maximum of 1500°C.[11] The exact temperature at which recrystallization negatively affects a refractory metal part is difficult to determine, as it depends on the the total time at a given temperature, the degree of cold-working the part has undergone prior to heating, and the presence of any impurities.[16] Temperature measurements of the aforementioned tungsten wire heaters during operation found that the heater coil was reaching 1800°C,[4] meaning that recrystallization was almost certainly complete. This temperature is also beyond the recommended use temperature for alumina, and boron nitride begins to react with bulk tungsten at 1600°C.[17] Given the tendency of the refractory metals for material interactions and degradation of properties at high temperature, it appears that their use should be avoided for a reliable high-power heater design.

To address the shortfalls of legacy and refractory-metal heaters for high-power heating of large hollow cathodes, we have designed, implemented, and tested a graphite heater capable of delivering multiple kilowatts of heater power with an estimated operational life of over 40 years. Section II outlines general guidelines for the design of a graphite heater for large hollow cathodes, including materials selection, geometry, and numerical prediction of operating temperature, power requirement, and operational life. As part of the design procedure, we have developed two models to predict the temperature and resistance of the graphite heater, a simplified circuit model and a finite-element model using COMSOL multiphysics software. Two vacuum sublimation models are also used to estimate heater life. Physical implementation and experimental tests of a graphite heater for a large hollow cathode at input powers of up to 4.5 kW are presented in Section III. Experimental results are then compared with the numerical predictions to validate the design process.

II. Graphite Heater Design

A. Material Considerations

1. Heater Element

A graphite cathode heater presents numerous advantages over swaged-tantalum or refractory-wire heaters. The work function of graphite, 5.0 eV, is higher than those of the refractory metals[18] and it is therefore less likely to act as a secondary cathode during heater operation, thus discouraging plasma attachment to the heater. The sputtering yield of graphite is also lower than those of both molybdenum and tantalum,[6,18–20] hence reducing erosion of the heater by the discharge plasma. In vacuum at the temperatures required for large cathode ignition — on the order of 1300 to 1500°C[4] — the main life-limiting mechanism for the graphite heater is sublimation rather than melting or chemical interaction. This further prevents shorting of the heater to other cathode components. Graphite is also chemically compatible with the design of state-of-the-art large hollow cathodes, which rely principally on graphite and boron nitride. Graphite also provides a significant advantage over heater architectures that use alumina due to the substantially higher thermal shock resistance,[11,21] possibly allowing for faster start up and cathode ignition. Finally, graphite is lightweight, abundant, easily machined, and its mechanical properties do not degrade after exposure to very high temperatures. Depending on the grade of material used, graphite becomes stiffer and stronger with increasing temperature.[22] These combined characteristics make graphite a very attractive material for high-power, long-life heater operation.

2. Electrical Leads

The main heater body is connected to the power supply through high-temperature stainless steel bars that serve as electrical leads. The grade of stainless steel should be electrically conductive and maintain its strength at high temperatures while offering low thermal conductivity to help reduce the heat lost by conduction through the electrical leads. The steel is subsequently connected to copper wiring which is then connected to the heater power supply. This approach prevents direct contact between copper and graphite while maintaining low electrical resistance. At the required operating temperatures, copper would likely melt on contact with the heater tabs and its thermal conductivity would also increase conduction losses through the electrical leads.

B. Heater Geometry

The heater dimensions are chosen to cover the exterior of the cathode tube over the length of the emitter region, while sliding over the electrical insulation surrounding the cathode tube. The flat "pseudo-coil" pattern shown in Figure 1 of the heater element was chosen as it allows for the appropriate resistance at the desired operating temperature while being simple to machine. This design also allows for thermal contact between the heater and the cathode over a large area, and the axial band structure helps in promoting uniform temperatures along the length of the cathode tube. The number of "coils" was chosen for ease of manufacturing and structural stiffness of the heater bands. A Computer-Aided-Design (CAD) drawing of the corresponding heater with 4 pseudo-coils is shown in Figure 2. Throughout this paper, we will use the term "band" to refer to the long axial sections of the graphite heater, "tab" to refer to the radial protrusions used as electrical leads, "gap" to refer to the open sections of the heater between bands, and the term "thickness" will be used to refer to the radial thickness of the heater bands.

This heater design is simple to analyze, and can be tailored to fit the desired cathode dimensions and required heater powers, as the number of coils along with the band thickness and width can be adjusted freely so long as the heater remains structurally stable. For example, if a longer cathode were to be used, the heater axial length could be increased and the band thickness increased to maintain the same resistance.

C. Heater Performance

1. Simplified Circuit Model

Knowledge of the graphite heater resistance is necessary in order to choose an appropriate power supply and to determine the required current and voltage to achieve the desired operating temperature. A simplified circuit model can be used to estimate the resistance of the heater at a given operating temperature, and

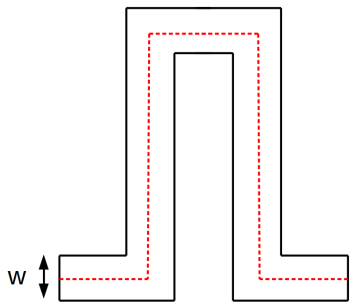

Figure 1. Pseudo-coil of width w, thickness t. The dashed line indicates the total length, L.

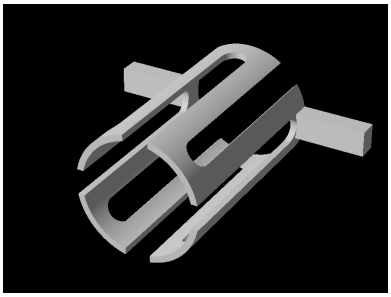

Figure 2. CAD rendering of the proposed heater with 4 pseudo-coils.

if the cathode heater power requirement for ignition — which can be estimated using any suitable thermal model of the cathode heat losses or prior experiment — is known, then the equilibrium temperature can also be estimated by imposing a power supply voltage across the heater element. The resistance and power output of the graphite heater for a given operating temperature T and power supply voltage V_s are estimated by a simplified model that treats each pseudo-coil as a resistor with a constant cross-sectional area — i.e., the variations in cross section at the turning points of the heater bands are ignored. N pseudo-coils can then be modeled by two resistors of value R_{half} in parallel, corresponding to the top and bottom halves of the heater. The equivalent resistance R is obtained by considering each pseudo-coil as a single resistor of resistance R_{pc}:

$$R_{\text{half}} = \frac{N}{2} R_{pc}(T) \rightarrow R(T) = \frac{N}{4} R_{pc}(T). \tag{1}$$

Since the cross-section of the graphite heater along each coil is assumed constant, each pseudo-coil is modeled as a homogeneous graphite bar of total length L, thickness t, and width w. Hence, R_{pc} is given by:

$$R_{pc}(T) = \frac{\rho(T) L}{tw}, \tag{2}$$

where $\rho(T)$ is the resistivity of graphite as a function of temperature.

Assuming that the heater has a uniform temperature and ignoring the effect of thermal expansion, we derive a constant "shape factor" from Equations 1 and 2, which depends only on geometry:

$$s = \frac{R(T)}{\rho(T)} = \frac{N}{4} \frac{L}{tw}. \tag{3}$$

The heater power delivered at a given temperature and power supply voltage is then readily obtained:

$$P_{\text{heater}} = \frac{V_s^2}{R(T)} = \frac{V_s^2}{s\rho(T)}. \tag{4}$$

The equilibrium temperature can then also be obtained by matching the heater power delivered as a function of temperature, $P_{\text{heater}}(T)$ with the cathode thermal loss power as a function of temperature (which

must be obtained via a separate model). Given the availability of COMSOL for combined thermal and electrical modeling, we do not use the simplified model to predict equilibrium temperature, only heater resistance.

2. Finite-Element Approach

Finite-element simulations of the graphite heater have been conducted using COMSOL Multiphysics software to obtain the average surface temperature of the heater for a given input power, the corresponding electrical resistance, and the temperature distribution of the heater along the emitter length. These values are necessary to predict whether cathode ignition can be achieved at a given power and to estimate the heater life.

Given the two axes of symmetry present in the heater design, we restrict the simulation domain to one quarter of the full 3D heater geometry. During operation, the heater temperature is expected to be controlled by Joule heating in the graphite and radiation losses from the outward-facing radial surfaces of the heater element. Imposing radiation-to-ambient boundary conditions on these surfaces, and half the available power supply voltage between the electrical lead surface and the vertical symmetry axis, we can predict the maximum current flowing through the heater and the heater temperature. For steady-state operation, we assume that the cathode and the heater have reached a uniform temperature, and that conduction losses to the back of the cathode and electrical leads can be ignored; in this configuration, we need only consider the heat radiated from the outer surface as the primary heat loss mechanism. Thermal and electrical conductivities and surface emissivity as functions of material temperature from Refs. 22 and 23 are incorporated into the model. A typical temperature profile of the heater obtained from the COMSOL model is shown in Figure 3.

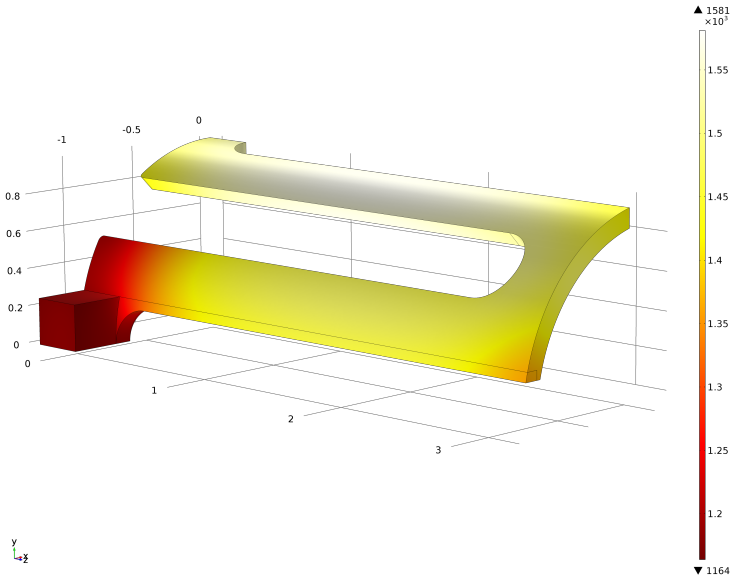

Figure 3. Typical heater temperature profile (°C). Obtained at 5.2 kW of heater power (V=21 V, I=247 A). Grid dimensions are in inches.

D. Lifetime Estimation

The machined graphite heater is flexible at room temperature, and is ideally only constrained by the electrical leads and cathode tube insulation. Under the assumption that the graphite heater can withstand any static structural forces it is subjected to while cold, the increase in strength and stiffness with temperature[21,22,24] of the grade of graphite used allows us to expect that the only likely failure mode of the heater is reduction of the heater thickness by carbon sublimation.

To compute the lifetime of the graphite heater, we rely on vapor pressure data available for carbon for the operating temperatures of interest, and follow two approaches to calculate the sublimation mass flux of graphite in vacuum.

1. Sublimation Mass Flux

Hertz-Knudsen Approach Though the dominant evaporant species from graphite in vacuum depends on temperature,[25] we assume a worst-case scenario in which atomic carbon is the main species sublimated. Using the experimental data from Ref. 26, we consider a sticking/evaporation coefficient, α_v, equal to unity. The evaporation mass flux Γ from an area A_s at temperature T for a particle of mass m with equilibrium vapor pressure P_v is given by the Hertz-Knudsen law:

$$\Gamma = \frac{1}{A_s}\frac{dm}{dt} = \alpha_v \frac{(P_v - P)}{\sqrt{2\pi m k_B T}} m. \tag{5}$$

In order to predict the mass loss rate per unit surface area, we also assume that the heater is operating in high vacuum. Therefore, P is negligible. The vapor pressure in Torr, P_v, for carbon at temperature T in Kelvin is given by:[27]

$$\log_{10} P_v = 16.811 - \frac{37940}{T} + 9.64 \times 10^{-4} T - 1.95 \log_{10} T. \tag{6}$$

Thieberger Approach In the approach outlined in Ref. 28, the upper limit of the mass flux Γ emitted from the heater surface is given by:

$$\Gamma = \frac{\rho \bar{c}}{4}, \tag{7}$$

where $\bar{c}$ is the average thermal velocity of the evaporating particles, and ρ is the mass density calculated using the ideal gas law and the vapor pressure from Equation 6. The average velocity is obtained by assuming a Maxwellian distribution of particles.

2. Lifetime Calculation

The recession velocity v_s of the heater surfaces is subsequently derived from the mass flux per unit area Γ obtained in Equation 5 or Equation 7, and the mass density ρ_g of graphite:

$$v_s = \frac{\Gamma}{\rho_g}. \tag{8}$$

The 1% loss life of the heater is then calculated using the recession velocity, v_s, and the band thickness, t:

$$\tau_{\max} = t/v_s \cdot 1/100. \tag{9}$$

III. Results and Discussion

Numerical and experimental results are based on the large LaB_6 hollow cathode presented in Ref. 4, which features a 2.7-inner-diameter, 8-cm-long LaB_6 emitter and a graphite cathode tube.

A. Implementation

Table 1 contains the nominal dimensions of the designed heater. Figure 4 shows the corresponding machined graphite heater, fabricated from grade AXM-5Q POCO graphite. The tabs are electrically connected to two, 2/0 copper wires in parallel via four, 1/2-inch-wide by 1/4-inch-thick by 6-inch-long high-temperature 253MA stainless steel bars. The 253MA stainless steel satisfies the requirements delineated in Section II.A.2.[29] Each pair of leads is held together with two 1/4"-20 bolts to provide good electrical contact with the graphite tabs. The emitter portion of the cathode tube is insulated by three molybdenum sheet heat shields to reduce radiative losses. While more layers of insulation would be ideal, three layers allow for continued diagnostics access to the heater and cathode tube. Boron nitride insulators enclose the graphite tabs to prevent any electrical connection between the heater and the molybdenum heat shields. The final setup with and without molybdenum heat shields is shown in Figure 5.

Table 1. Nominal dimensions of the heater.

Dimension	Value (in.)
Axial length	3.20
Inner diameter	1.75
Outer diameter	1.95
Band width	0.294
Band thickness	0.100
Gap width	0.394
Tab length	1.00
Tab width	0.394
Tab height	0.394

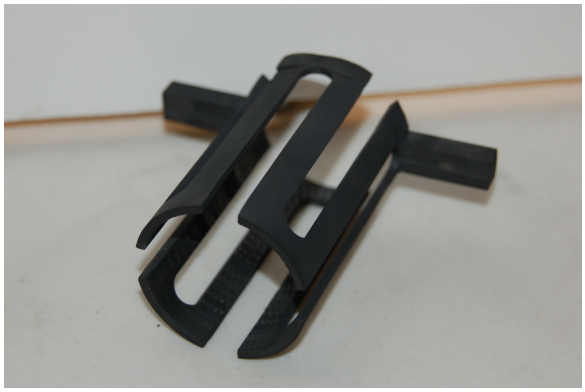

Figure 4. Finished graphite heater.

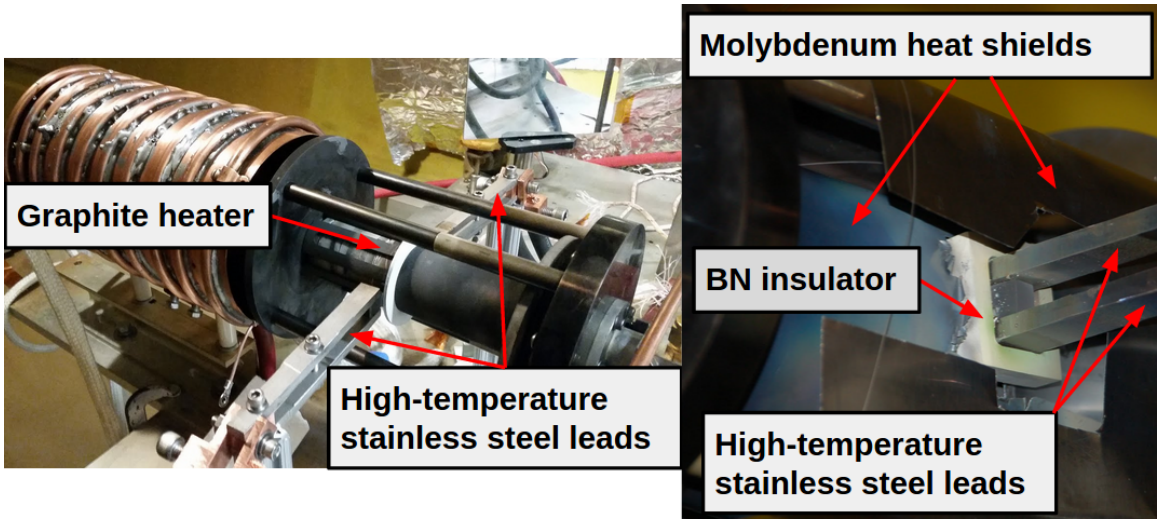

Figure 5. Graphite heater installed on hollow cathode without heat shields (left). Detail of the boron nitride insulator with heat shields installed (right).

B. Experimental Results

1. Apparatus

The cathode is installed in a 2 m-diameter by 5 m-length vacuum vessel, evacuated to pressures in the 6×10^{-5} Torr range. Temperature measurements were taken during the cathode start-up stage using a

thermocouple installed on the outward radial surface of the tip of the cathode tube and a Leeds & Northrup Model 8622-C optical pyrometer aimed manually at the exposed portion of the heater tip. The graphite heater is powered by an American Reliance 32V/400A power supply.

2. Operating Temperature and Heater Resistance

The numerical approach is validated by comparing it to experimental operating temperature and heater resistance. Correct numerical predictions allow for fast estimation of operating temperature and provide important information for heater life estimation, as well as power requirements of a heater design for a large hollow cathode.

Thermocouple and optical pyrometer data for the cathode tip and heater element temperatures for various input powers are shown in Figure 6, along with the surface-averaged temperatures obtained with the finite-element approach for the corresponding heater power. Pyrometric data below 760°C are not available as these temperatures are outside the range of our optical pyrometer. The predicted heater resistances from the circuit model and the finite-element approach are shown in Figure 7 along with those calculated from the experimental data using either the thermocouple or pyrometer temperature measurements.

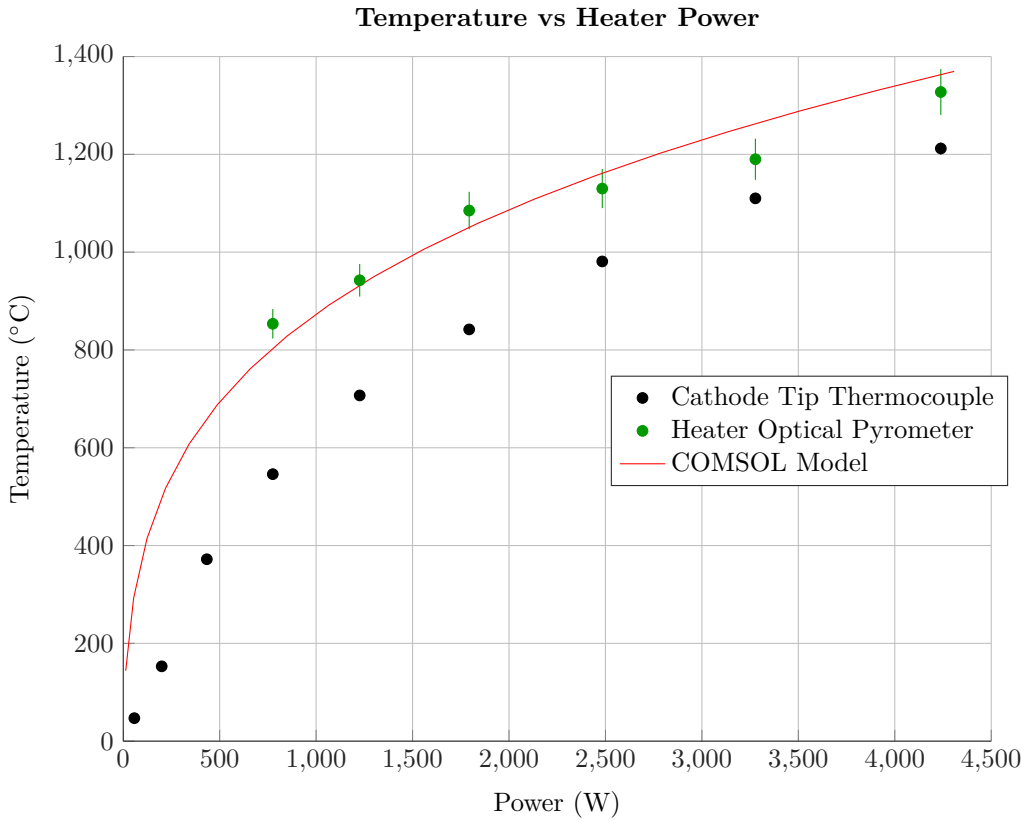

Figure 6. Temperatures of the cathode tip and heater element versus input heater power. The surface-averaged heater temperatures predicted by the COMSOL model are also shown versus input power.

Experimental and numerical data of the operating temperature of the tip of the cathode follow an identical trend. Furthermore, the finite-element approach agrees well with the pyrometric readings.

Both sets of experimental heater resistance data were found to follow the same trend as the predictions of the circuit and finite-element models; the resistance decreases for temperatures lower than 500°C, followed by an approximately linear increase. The offset in the minimum resistance of the circuit model is caused by the assumption of uniform temperature in that model. The circuit model also over-estimates the resistance calculated using the heater pyrometer data by about 15%, and over-estimates the resistance found using the thermocouple data by 41% at low temperature with the error decreasing to about 12% as the temperature increases to 1200°C. It could simply be the case that since the heater resistance is driven by the heater temperature and not the cathode temperature, the pyrometer data is more representative of the heater

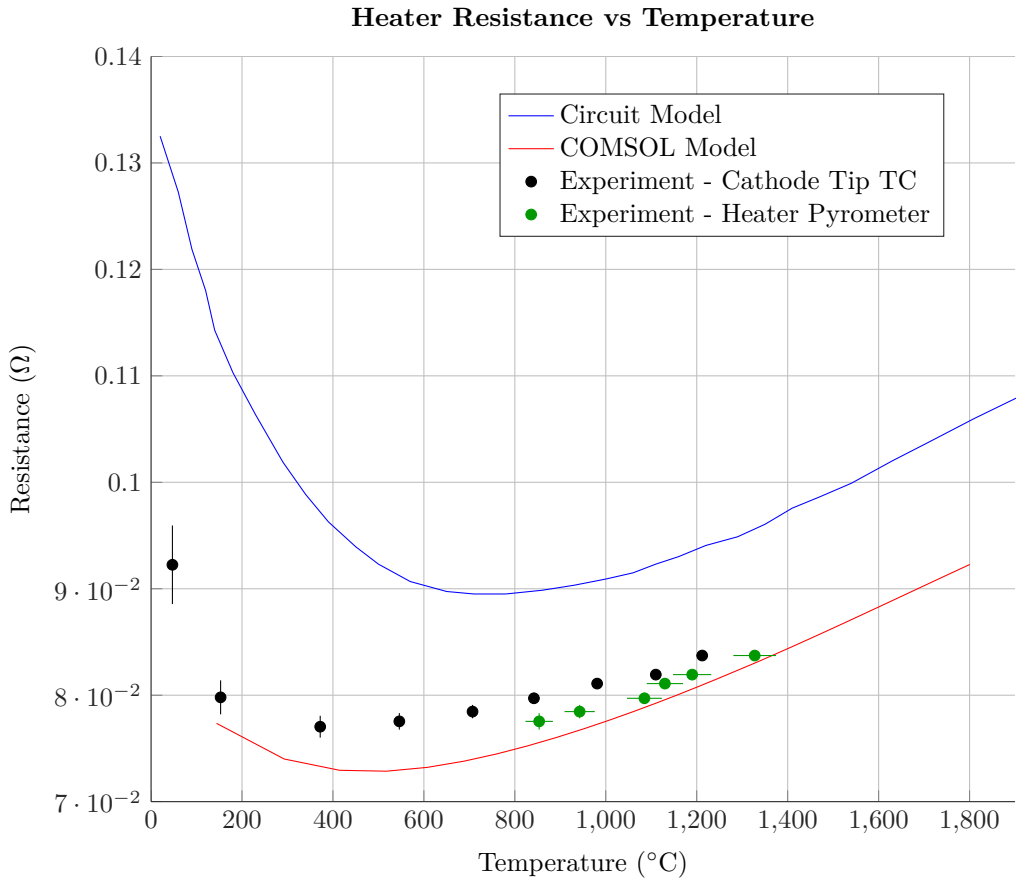

Figure 7. Heater resistance as a function of temperature, calculated using the circuit model, finite element model, and each set of experimental temperature measurements.

behavior. Given the simplicity of the circuit model, this level of agreement with the experimental data is still encouraging for use as a rapid design tool. The finite-element approach agrees well with the pyrometer data at high-temperatures, though it overestimates the actual power necessary to achieve a given temperature. The lack of shielding in the finite-element approach may explain the lower temperature observed for a given input heater power. The agreement of the COMSOL model with the experimental data unfortunately also suggests that either the molybdenum heat shields are not very effective at shielding the cathode (though many more layers of insulation would certainly be used in a flight-model cathode), or that the conduction losses in the cathode are high enough to compensate for the error introduced by the lack of heat shielding in the COMSOL model.

3. Planned Improvements

The graphite heater element itself could provide up to 11 kW of input power with the power supply available, but our measurements are currently limited to 4.5 kW. This limitation comes from the melting of the steel electrical leads at input currents above 230-240 A. The current cathode can be repeatably ignited using the heater in its current form, but reduction of the required power by improved shielding is certainly desirable, and removing the temperature limitation imposed by the electrical leads would demonstrate that this heater architecture is suitable for even higher power operation. Further iterations of the heater will use tungsten or titanium carbide leads in lieu of the high-temperature stainless steel; tungsten carbide has a melting point of 2,777°C and titanium carbide melts at over 2,940°C.[12] Though pure refractory metals are prone to failure as described in Section I, the refractory carbides do not exhibit the same problems and do not react with graphite at high temperature in vacuum.[30]

C. Lifetime estimation

The 1% loss life of the heater with the dimensions given from each of the two approaches delineated in Section II.D is shown in Figure 8. The two models provide almost identical results, and predict a lifetime of approximately 400 kh for a graphite heater with the specified geometry operating continuously at 1,500°C. Considering that this operational life is a very conservative estimate, this heater architecture is very promising for any long-term mission.

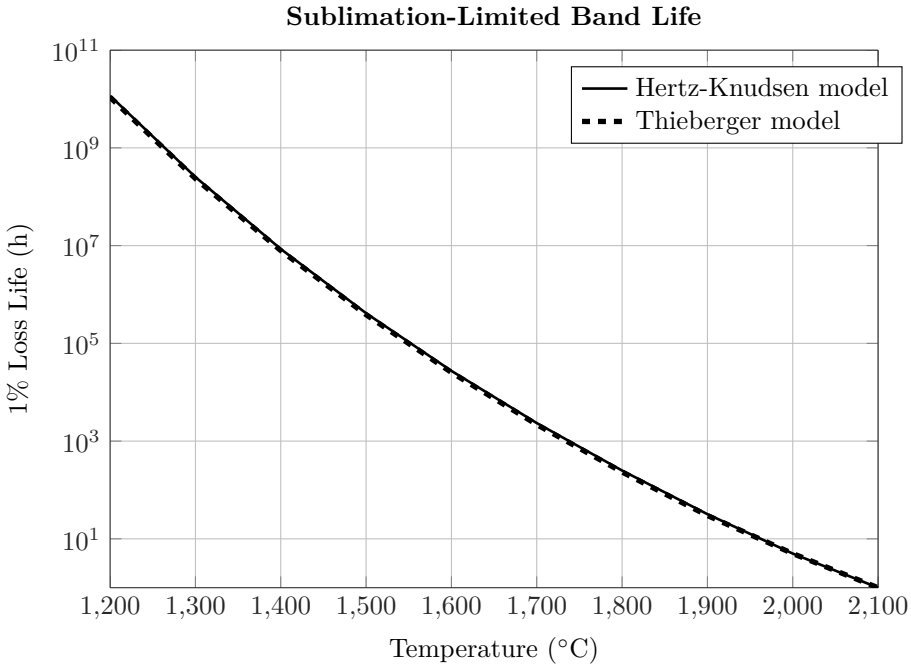

Figure 8. Estimated heater lifetime as a function of operating temperature. Lifetime is given by the time required for sublimation of 1% of the heater band thickness.

IV. Conclusion

We have designed a multiple-kilowatt graphite heater for large thermionic hollow cathodes in order to address growing heater power needs and the life issues facing swaged-tantalum and refactory-metal-based heaters at high-power operation. Use of the design procedure and life estimation methods described should allow for graphite heaters to be used for a wide range of cathode sizes, eliminating the material problems engendered by existing heater designs and allowing for an order-of-magnitude increase in available heater power.

Ignition of the prototype 2.7-cm-inner-diameter hollow cathode was achieved repeatably using the graphite heater described in the preceding sections while operating at 4.5 kW of heater power and a temperature of 1,328°C as measured on the exposed surface of the heater element by optical pyrometry.Even higher heater power could be achieved by replacing the stainless steel electrical leads with refractory carbide materials; the only current limitation was localized melting of the electrical leads.No degradation of the performance of the heater has been detected otherwise. A simple circuit model of the heater along with a finite-element simulation of the heater agree reasonably well with experimental data. The circuit model provides a very simple and rapid design tool for graphite heaters for different cathode sizes.

The principal predicted life-limiting mechanism for the graphite heater is reduction of the element thickness by carbon sublimation. We have presented two approaches for estimating the evaporation losses from the heater surface and both methods conservatively estimate extremely long heater life. The heater has an estimated 1% material loss life of 400 kh — over 40 years of continuous operation — at 1,500°C. The power and operational life provided by this graphite heater design should be more than sufficient to satisfy the needs of next-generation cathodes for high-power Hall thrusters, and the design is easily modified for different cathode sizes.

Acknowledgments

This work was supported by the U.S. Air Force Office of Scientific Research under grant number FA9550-11-1-0241. The authors would like to thank Bob Sorenson for his technical support.

References

[1]Brown, D. L., et al., "Air Force Research Laboratory High Power Electric Propulsion Technology Development," IEEE Aerospace Conference, 2009, doi: 10.1109/AERO.2010.5447035.

[2]Goebel, D. M. and Chu, E., "High Current Lanthanum Hexaboride Hollow Cathodes for High Power Hall Thrusters," International Electric Propulsion Conference, 2011, doi: IEPC-2011-053.

[3]Hofer, R.R., et al., "Evaluation of a 4.5 kW Commercial Hall Thruster System for NASA Science Missions," Joint Propulsion Conference, 2006, doi: 10.2514/6.2006-4469.

[4]Plasek, M. L., et al., "Experimental Investigation of a Large-Diameter Cathode," Joint Propulsion Conference, 2014, doi: 10.2514/6.2014-3825.

[5]Goebel, D. M. and Chu, E., "High-Current Lanthanum Hexaboride Hollow Cathode for High-Power Hall Thrusters," Journal of Propulsion and Power, 2014, doi: 10.2514/1.B34870.

[6]Chu, E., et al., "Reduction of Energetic Ion Production in Hollow Cathodes by External Gas Injection," Journal of Propulsion and Power, 2013, doi: 10.2514/1.B34799.

[7]Goebel, D. M. and Chu, E., "High Current Lanthanum Hexaboride Hollow Cathode for 20-100 kW Class Hall Thrusters," Joint Propulsion Conference, 2012, doi: 10.2514/6.2012-4079.

[8]Goebel, D. M. and Watkins, R. M., "Compact Lanthanum Hexaboride Hollow Cathode," Review of Scientific Instruments, 2010, doi: 10.1063/1.3474921.

[9]Mathers, A., "Development of a High Power Cathode Heater," Joint Propulsion Conference, 2008, doi: 10.2514/6.2008-4815.

[10]Tighe, W. G., et al., "Performance Evaluation and Life Test of the XIPS Hollow Cathode Heater," Joint Propulsion Conference, 2005, doi: 10.2514/6.2005-4066.

[11]Thermo-Shield, "Typical Properties of Materials," http://www.thermoshield-us.com/pdf/Copy-of-material-properties-chart-w-Ceramics.pdf.

[12]Cardarelli, F., Materials Handbook, 2nd Edition, Springer, 2008, doi: 10.1007/978-1-84628-669-8.

[13]English, J. J., "Binary and Ternary Phase Diagrams of Columbium, Molybdenum, Tantalum, and Tungsten," Tech. Rep. Report 152, Defense Metals Information Center, 1961.

[14]Rudy, E., "Ternary Phase Equilibria in Transition metal-boron-carbon-silicon systems," Tech. Rep. AFML-TR-65-2, Air Force Materials Laboratory, 1969.

[15]Xiong, W., et al., "Thermodynamic assessment of the Mo-Nb-Ta system," Computer Coupling of Phase Diagrams and Thermochemistry, Vol. 28, 2004.

[16]Patee, H. E. and Evans, R. M., "Brazing and Bonding of Columbium, Molybdenum, Tantalum, Tungsten, and Graphite," Tech. Rep. Report 153, Defense Metals Information Center, 1962.

[17]Lassner, E. and Schubert, W., Tungsten, Springer Science+Business Media, LLC, 1999, doi: 10.1007/978-1-4615-4907-9.

[18]Lide, D. R., Handbook of Chemistry and Physics, 77th ed., CRC Press, 1997.

[19]Mantenieks, M. A., et al., "Low Energy Xenon Ion Sputtering Yield Measurements," International Electric Propulsion Conference, 2001.

[20]Doerner, R. P., et al., "Sputtering Yield Measurements During Low Energy Xenon Plasma Bombardment," Journal of Applied Physics, Vol. 93, No. 9, 2003, doi: 10.1063/1.1566474.

[21]Entegris, "Properties and Characteristics of Graphite," 2013.

[22]Poco Graphite Inc., "Properties and Characteristics of Graphite For Industrial Applications," 2001.

[23]Cezairliyan, A. and Miller, A. P., "Heat Capacity and Electrical Resistivity of POCO AXM-5Q1 Graphite in the Range 1500-3000 K by a Pulse-Heating Technique," International Journal of Thermophysics, Vol. 6, No. 3, 1985, doi: 10.1007/BF00522150.

[24]Poco Graphite Inc., "Properties and Characteristics of Graphite For the EDM Industry," 2002.

[25]Zavitsanos, P. D. and Carlson, G. A., "Experimental study of the sublimation of graphite at high temperatures," Journal of Chemical Physics, Vol. 59, 1973, doi: 10.1063/1.1680430.

[26]Paul, B., "Compilation of Evaporation Coefficients," ARS Journal, 1962, doi: 10.2514/8.6277.

[27]Setton, R., "Carbon, A Fundamental Element for Research and Its Applications," Carbon Molecules and Materials, CRC Press, 2002, doi: 10.1201/b16832-2.

[28]Thieberger, P., "Upper Limits for Sublimation Losses from Hot Carbon Targets in Vacuum and in Gases," 2000, www-mucool.fnal.gov/mcnotes/public/pdf/muc0186/muc0186.pdf.

[29]Rolled Alloys, "RA 253 MA Data Sheet," 2012, http://content.rolledalloys.com/technical-resources/databooks/RA253-MA_DB_US_EN.pdf.

[30]Burykina, A. L. and Evtushok, T. M., "The Contact Interaction of Metal-Like Carbides with Graphite at High Temperatures in a Vacuum," Poroshkovaya Metallurgiya, Vol. 2, No. 20, 1964, doi: 10.1007/BF00774477.